

## SPATIALLY RESOLVED 3 $\mu\text{m}$ SPECTROSCOPY OF ELIAS 1: ORIGIN OF DIAMONDS IN PROTOPLANETARY DISKS<sup>1</sup>

M. GOTO,<sup>2</sup> TH. HENNING,<sup>2</sup> A. KOUCHI,<sup>3</sup> H. TAKAMI,<sup>4</sup> Y. HAYANO,<sup>4</sup> T. USUDA,<sup>4</sup> N. TAKATO,<sup>4</sup> H. TERADA,<sup>4</sup> S. OYA,<sup>4</sup> C. JÄGER,<sup>5</sup> A. C. ANDERSEN<sup>6</sup>

*Draft version October 30, 2018*

### ABSTRACT

We present spatially resolved 3  $\mu\text{m}$  spectra of Elias 1 obtained with an adaptive optics system. The central part of the disk is almost devoid of PAH emission at 3.3  $\mu\text{m}$ ; it shows up only at 30 AU and beyond. The PAH emission extends up to 100 AU, at least to the outer boundary of our observation. The diamond emission, in contrast, is more centrally concentrated, with the column density peaked around 30 AU from the star. There are only three Herbig Ae/Be stars known to date that show diamond emission at 3.53  $\mu\text{m}$ . Two of them have low-mass companions likely responsible for the large X-ray flares observed toward the Herbig Ae/Be stars. We speculate on the origin of diamonds in circumstellar disks in terms of the graphitic material being transformed into diamond under the irradiation of highly energetic particles.

*Subject headings:* circumstellar matter — dust, extinction — planetary systems: protoplanetary disks — early-type — stars: formation — stars: individual (Elias 1)

### 1. INTRODUCTION

Spatially extended PAH emission, but confined to a protoplanetary disk (Habart, Natta, & Krügel 2004; van Boekel et al. 2004; Geers et al. 2007; Doucet et al. 2007), provides crucial evidence for the two-layer disk model consisting of a cold mid-plane and a warm disk atmosphere (Men'shchikov & Henning 1997; Chiang & Goldreich 1997; Dullemond, Dominik, & Natta 2001). More detailed studies on PAH chemistry coupled with advanced disk modeling may provide a powerful tool for using PAH emission to better understand the evolution and structure of protoplanetary disks (Visser et al. 2007; Dullemond et al. 2007). However, the emission feature at 3.53  $\mu\text{m}$  observed in the spectra of several Herbig Ae/Be stars has been an enigma since its discovery in the 1980s (Whittet et al. 1983; Whittet, McFadzean, & Geballe 1984). Many explanations have been proposed (Schutte et al. 1990; Allamandola et al. 1992), until Guillois et al. (1999) conclusively identified small diamond particles as the carrier of the emission (Sheu et al. 2002; Jones et al. 2004). Despite extensive investigation (e.g., van Kerckhoven, Tielens, & Waelkens 2002; Habart et al. 2004; Topalovic et al. 2006), the origin of diamonds in protoplanetary disks remains essentially inconclusive, except that they are likely not of interstellar origin but are formed close to the star.

Electronic address: mgoto@mpia.de

<sup>1</sup> Based on data collected at Subaru Telescope, which is operated by the National Astronomical Observatory of Japan.

<sup>2</sup> Max Planck Institute for Astronomy, Königstuhl 17, D-69117 Heidelberg, Germany.

<sup>3</sup> Institute of Low Temperature Science, Hokkaido University, Sapporo 060-0819, Japan.

<sup>4</sup> Subaru Telescope, 650 North A'ohoku Place, Hilo, HI 96720, USA.

<sup>5</sup> Institut für Festkörperphysik, Friedrich-Schiller-Universität Jena, Helmholtzweg 3, D-07743 Jena, Germany.

<sup>6</sup> Dark Cosmology Centre, Niels Bohr Institute, University of Copenhagen, Juliane Maries Vej 30, DK-2100 Copenhagen, Denmark.

Elias 1 (V 892 Tau) is a Herbig Ae/Be star located in the Taurus-Auriga complex at a distance of  $140 \pm 20$  pc (Elias 1978), with an estimated age younger than 3 Myr (Strom & Strom 1994). The geometry of the disk is poorly known. A large infrared excess is still present in the far-infrared spectral energy distribution, indicating flaring in the outer part of the disk (Meeus et al. 2001). Near-infrared speckle observations detected a possible elongation of 40 to 100 AU from east to west (Kataza & Maihara 1991). However, whether it represents a disk or a scattered bipolar lobe is still an open question (Haas, Leinert, & Richichi 1997). The source is unresolved at sub-mm wavelengths, leaving little useful information as to the inclination or the disk position angle (Henning et al. 1998; di Francesco et al. 1997). However, recent mid-infrared nulling interferometry observations give a preliminary disk diameter of 20–30 AU at 10  $\mu\text{m}$  (Liu et al. 2007).

### 2. OBSERVATIONS

Long-slit spectroscopy was performed at the Subaru Telescope on September 12, 2003, using the facility spectrograph IRCS (Tokunaga et al. 1998; Kobayashi et al. 2000) together with a curvature-sensing adaptive optics system optimized for nearly diffraction-limited imaging at wavelengths longer than 2  $\mu\text{m}$  (Takami et al. 2004). The medium-resolution grism was used with a reflective slit of  $0'.3 \times 20''$  to provide spectra with a resolving power of  $R = 1,000$ . The slit was oriented in two directions, one east-to-west parallel to the major axis of the elongation of the disk suggested by Kataza & Maihara (1991), and one perpendicular to this direction. The spectra were recorded by moving the tip-tilt mirror inside the adaptive optics system by  $3''$  along the slit for sky subtraction. The amplitude of dithering virtually defined the outer boundary of our observation. Extra caution was taken to center the object in the slit in order to prevent recording the point spread function (PSF) in its wings. The short integration time of 2 s was repeated 10 times for one exposure to avoid detector saturation. The spec-

tra of the standard star HR 1490 ( $V = 5.8$  mag; A2V) were obtained immediately after Elias 1, also with the adaptive optics system. The standard star was dimmed by the neutral density filters in front of the wavefront sensor so that the residual wavefront error was as similar as possible to that of Elias 1 ( $V = 15.3$  mag).

### 3. DATA REDUCTION AND RESULTS

#### 3.1. Spectral extraction

Two-dimensional images of the spectra were reduced separately frame by frame in order not to smear out the spatial resolution. After preliminary processing, including pair subtraction and flat fielding, the centroid of the PSF was traced along the wavelength to set the aperture center of the spectral extraction. In total, 17 strips of spectra were extracted from one frame from the apertures set at every 10 AU ( $0''.07$ ) from the center up to 70 AU ( $0''.5$ ) on both sides of the star, and from one additional aperture at 100 AU (80–120 AU) at the outer edge. The aperture width ( $0''.07$ ) was set for a proper sampling of the PSF (FWHM  $\approx 0''.1$ ). However, it was about the same size as the pixel scale ( $0''.06$ ). The limited sampling of the PSF, together with a slight curvature of the spectra along the array column, sometimes causes an artificial wobbling of the spectral continuum. In order to minimize this effect, we extracted the same number of spectra from the standard star HR 1490 across its PSF and divided the spectrum of Elias 1 by the spectrum of HR 1490, extracted from the same aperture with the same offset from the center. The wavelength calibration was performed by matching the telluric absorption lines to the model transmission curve computed by ATRAN (Lord 1992). A set of spectra extracted from different frames, but at the same aperture were finally combined, and the dispersion of the spectra was taken as the error of the observation (Figure 1 and 2).

From the data, it is obvious that the PAH emission is relatively weak in the center (note that the pointed feature at  $3.3 \mu\text{m}$  is from Pf  $\delta$ ). The trend is identical for the east-to-west and the north-to-south directions. The spatial variation at a physical scale of about 10 AU already indicates that the PAH emission indeed arises from the circumstellar disk and not from a large envelope.

The spatial extension of the diamond emission is less obvious. We double checked the spatial profile of the diamond emission with respect to the continuum emission (Figure 3). The FWHM of the monochromatic PSF at the diamond feature is apparently larger than the one at the neighboring continuum emission. If we deconvolve the diamond emission with the continuum PSF, we could set the minimum size of the diamond emitting zone to 8–15 AU.

#### 3.2. Surface density

The absolute line flux was calibrated with respect to the standard star HR 1490, as Elias 1 itself is apparently extended, and the loss at the slit transmission is uncertain. For the calculation of the surface density of the PAH molecules, we assumed that all the energy absorbed in the UV to visible wavelengths is re-emitted in the infrared. Because we are more interested in the relative spatial variation, only a single size of PAHs was used

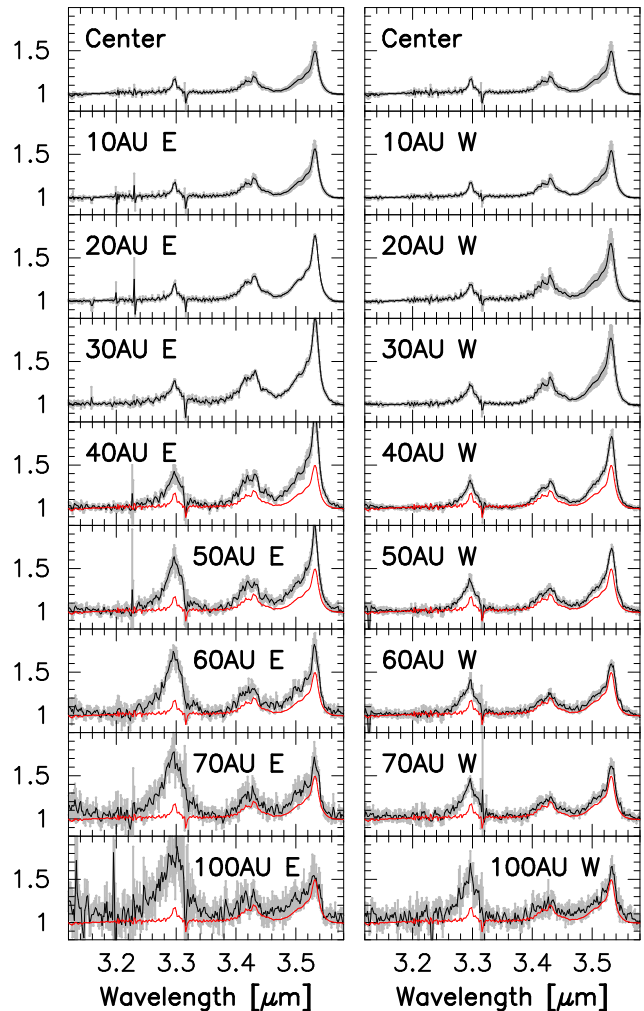


FIG. 1.— A spectral sequence across Elias 1 from east to west. The spectra were extracted every 10 AU from the star up to 70 AU, and at 100 AU (80–120 AU) at the outer boundary of the observation. The actual instrumental resolution is likely 20–30 AU. The red curves duplicate the spectra from the center to emphasize the variation. The error bars of the data points are given in gray. All spectra were normalized by the polynomial function, fitted to the continuum emission. The relative intensity of PAH emission ( $3.3 \mu\text{m}$ ) to diamond emission ( $3.53 \mu\text{m}$ ) becomes larger with distance, in particular in the outer region beyond 30 AU from the star. The pointed emission at  $3.3 \mu\text{m}$  in the central spectrum, much narrower than the PAH feature, is Pf  $\delta$ . The emission at  $3.42 \mu\text{m}$  is also from diamond, but from its defect.

in the calculation for simplicity. The absorption cross-section of a neutral PAH ( $a = 5.02 \times 10^{-4} \mu\text{m}$ ;  $N_C \approx 58$ ) was taken from Li & Draine (2001).

The spectral type of Elias 1 is uncertain, depending on how much foreground extinction is assumed, and varies from A6 (e.g., Cohen & Kuhi 1979) to B9 (Strom & Strom 1994). Here we take A6e from Thé et al. (1994) and use the photospheric model of A6V (Kurucz 1979) with the luminosity scaled to  $L_* = 56 L_\odot$  (Berrilli et al. 1992). No extinction of stellar radiation was applied along the line of sight. PAH molecules of this size are small enough to be heated stochastically. We refer to Draine & Li (2001) for the conversion of internal energy to the emitting temperature of the PAH molecules.

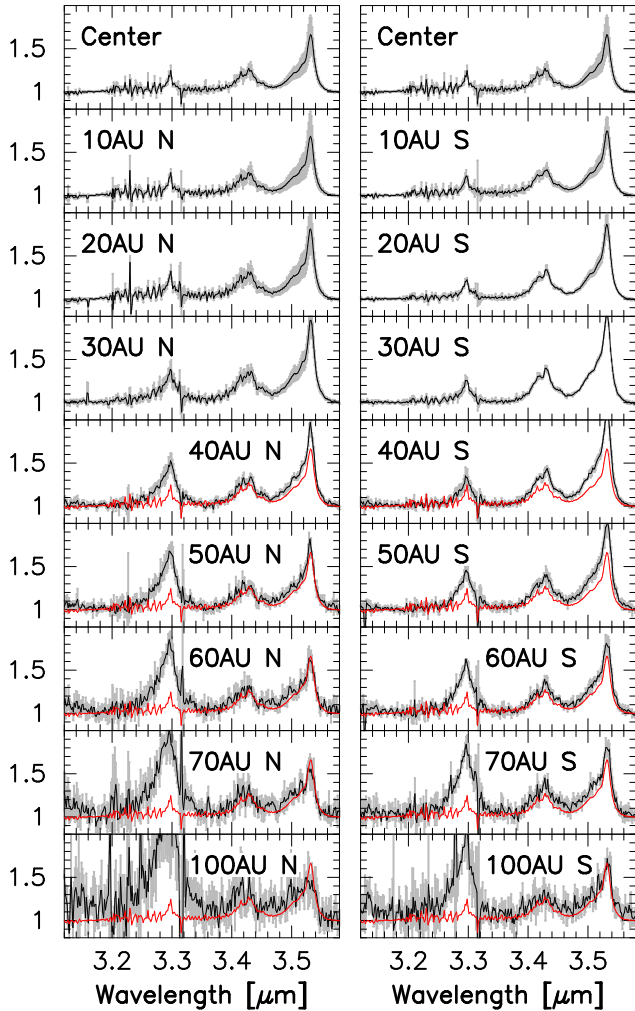


FIG. 2.— Same as Figure 1, but a spectral sequence along the north to the south. The same trend of the variation of PAH emission relative to the diamond is seen here.

The same calculation was repeated for diamonds, although the size of the diamond particles is still debated. The hydrogenation and the surface lattice structure require the temperature of diamond to be between 800 and 1000 K. van Kerckhoven, Tielens, & Waelkens (2002) argued that the particle has to be as small as 1–10 nm to consort with the range, as diamonds are poor emitter in the infrared, and larger particles become too hot and decompose themselves. However, the sheer appearance of the  $3.53 \mu\text{m}$  feature requires well-ordered crystal lattice of the physical scale of at least 25–50 nm (Sheu et al. 2002), or even larger (Jones et al. 2004). Here we assume a size of 100 nm, with the diamond particles being in equilibrium with the radiation. The absorption cross-section in the UV to the visible wavelengths is taken from Mutschke et al. (2004) and combined with that of hydrogenated diamond, which is responsible for the  $3.53 \mu\text{m}$  emission (Cheng et al. 1997). The spatial variation of the surface density of the PAH molecules and diamond particles is shown in Figure 4.

PAH molecules are much less abundant close to the star, within about 30 AU from the center. The abundance becomes higher with radial distance up to the

outer boundary of the observation. However, the diamond particles show a distinct spatial distribution from the PAHs and are more centrally concentrated but with peaks near 30 AU, where the PAH emission starts to emerge.

## 4. DISCUSSION

### 4.1. How Special Is a Diamond Emission Star?

There are only 3 Herbig Ae/Be stars known that have clear diamond signatures at  $3.53 \mu\text{m}$ : HD 97048 (Whittet et al. 1983), MWC 297 (Terada et al. 2001), and Elias 1 (Whittet, McFadzean, & Geballe 1984). An extensive survey conducted by Acke et al. (2006), covering more than 60 Herbig Ae/Be stars with  $3 \mu\text{m}$  spectroscopy, did not add a new source to the ones already known. However, the survey did find a few additional sources that might show the diamond features, such as T CrA, V 921 Sco, and HD 163296. There have been several reports of the detection of emission near  $3.5 \mu\text{m}$ , for instance HD 142527 by Waelkens et al. (1996) and HD 100546 by Malfait et al (1998). However, these newly found, or suggested, sources show relatively weak emission at  $3.5 \mu\text{m}$ , if any at all, but nothing comparable to those seen in the three Herbig Ae/Be stars listed above. The original paper of Whittet et al. (1983) that first reported the  $3.53 \mu\text{m}$  emission from Elias 1 and HD 97048 included TY CrA as another possible star that might show the same signature. However, the emission was not reproduced in later observations at the same wavelength (Acke et al. 2006). In contrast, the presence of diamond emission in Elias 1 and the other two Herbig Ae/Be stars has been demonstrated by multiple observations. We therefore take only these three sources as genuine detections. We discuss below if and how they are special and why they are so rare.

There are only two Herbig Ae/Be stars known thus far that have shown large X-ray flares: Elias 1 and MWC 297 (Giardino et al. 2004; Hamaguchi et al. 2000). Aside from the coincidence, this is intriguing, because Herbig Ae/Be stars are not supposed to be X-ray sources themselves. OB stars and young low-mass stars are soft and hard X-ray sources, respectively, due to the strong stellar winds and their magnetic activity (for a review Feigelson et al. 2007). In contrast, Herbig Ae/Be stars are too hot to maintain convective zones at the surface but are not luminous enough to set off strong stellar winds.

However, the X-ray flares from Elias 1 and MWC 297 have been reasonably accounted for by their low-mass companions. In addition to a T Tauri star at  $4''$  away (V 892 Tau NE; Giardino et al. 2004), Elias 1 was further resolved into two sources by bispectrum speckle interferometry (Smith et al. 2005). The newly found companion, only 50 mas or 7 AU away from Elias 1, is expected to have a mass in the range of  $1.5$  to  $2 M_{\odot}$ , very close, but within the upper limit of stellar mass that can still have a convective outer layer. Likewise, more than a handful X-ray sources cluster around MWC 297 (Damiani, Micela, & Sciortino 2006). One of the faint sources detected at  $H$  with an adaptive optics system at  $3'4$  away from MWC 297 is comparable to a T Tauri star in its brightness (Vink et al. 2005). The plasma temperature going up to  $\sim 8 \text{ keV}$  during the flare seen in

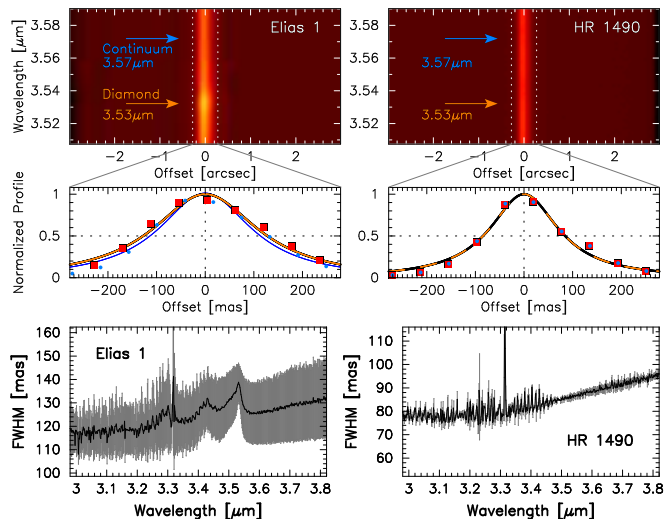


FIG. 3.— The spatial profile of the diamond emission. Top left and middle left: The diamond emission ( $3.53 \mu\text{m}$ ) is slightly extended compared to the continuum emission ( $3.57 \mu\text{m}$ ) right next to the emission features. Bottom left: The FWHM of the emission profiles measured along the wavelength. There is unambiguous enhancement of the FWHM at the PAH and the diamond features. Right: Same as the left panels, but for the standard star HR 1490. There is no trace of extended emission. If we take the FWHM of the nearby continuum (126 mas) to deconvolve the diamond profile (139 mas), the physical extension is 8 AU. If we instead take the FWHM of the standard star at the same wavelength (86 mas), it amounts to 15 AU. Note that the numbers represent the minimum extension of the diamond emission in both cases, where the emission feature contributes a substantial fraction of the flux at the wavelength comparable to the continuum emission.

Elias 1 (Giardino et al. 2004) indicates that it is caused by a similar mechanism for a solar flare. The unusual X-ray flares toward the Herbig Ae/Be stars are most likely attributable to the low-mass companions found recently (Stelzer et al. 2006).

HD 97048, the last Herbig Ae/Be star with diamond emission, is also known to be an X-ray source (Zinnecker & Preibisch 1994). No temporal variability of X-ray emission is reported. The search for very close companions is so far negative (e.g., Ghez et al. 1997). However, HD 97048 is among the hardest X-ray sources in Cha I cluster studied by XMM *Newton* (Stelzer et al. 2004). Along with the presence of nearby low-mass X-ray sources, it may imply that the circumstances are similar to those of Elias 1 and MWC 297.

Yet another example of a diamond signature is a post-AGB star, HR 4049 (Geballe et al. 1989). Although the evolutionary stage is totally different, it is tempting to note that the star’s spectral type is similar to that of the Herbig Ae/Be stars (B9.5 Ib-II); it also has a disk around (Dominik et al. 2003) and even a possible white dwarf companion as well (Lugaro et al. 2005).

A disk, a hot central star, and a companion emitting hard X-rays seem to be the conditions that “diamond stars” must have. The particular suite of conditions already suggests that the circumstellar environment plays a critical role in the formation of diamond, or at least the diamond features to appear. However, the nano-diamond particles found in meteorites are widely considered to be presolar origin, because of the isotope anomaly incompatible with that of solar system (Lewis et al 1987).

Searching sources of diamond outside the solar system is greatly in debt to the laboratory study of diamond formation facilitated by the interest from material science. Tielens et al. (1987) drew parallel between the synthesis of detonation diamond (e.g. Baidakova & Vul’ 2007) with possible diamond formation in the grain-grain collisions in the strong shocks in the ISM. Kouchi et al. (2005) used experimental simulation of the icy grains in the diffuse ISM to demonstrate diamond cores of nanometer size grow in the organic refractory in the UV irradiation.

Chemical vapor deposition (CVD) of diamond has been most extensively studied as the low-pressure path of diamond growth in the ISM. The CVD technique has been used to grow diamonds on the substrate in warm environment ( $\sim 1000 \text{ K}$ ) from hydrocarbon gas dissociated either by hot filaments or in a microwave cavity while protecting the growing surface in the hydrogen-rich atmosphere (for a review Angus & Hayman 1988; Frenklach et al. 1989b). Homogeneous nucleation relevant to the diamond formation in the ISM is also demonstrated in the laboratory by Frenklach et al. (1989a), although with chloride which is alien to the ISM but plays critical role in the enhancement of the nucleation rate (Asmann, Heberlein, & Pfender 1999). As the laboratory conditions of CVD experiments is similar to the physical conditions of atmosphere of carbon stars, much effort has been gone into linking the CVD diamond to astronomical observations (e.g. Wdowiak 1987; Andersen et al. 1998; Sheu et al. 2002) and to the nano-diamonds extracted from carbonaceous meteorites (Daulton et al. 1996). CVD diamond also inspired possible formation of diamond in supernova outbursts (Clayton et al. 1995; Nuth & Allen 1992). Jørgensen (1988) combined the two sources together, and tried to explain the isotope anomaly by a single binary system consisting of a carbon star and a white dwarf that eventually undergoes supernova outburst.

However, the laboratory conditions of CVD formation calls for an extreme carbon rich atmosphere in the standard of the ISM. A carbon star is a rare exception where the carbon abundance exceeds that of oxygen, and hydrocarbon molecules are copious in the environment. On the contrary, the ISM is intrinsically oxygen rich, so as a protoplanetary disk is. The abundance of carbon that Wdowiak (1987) refers is  $n(\text{C}) = 4 \times 10^{13} \text{ cm}^{-3}$  in the expanding atmosphere of the pressure  $10^3 \text{ dyn cm}^{-2}$  where  $n(\text{H})/n(\text{C}) = 200$ . On the other hand, the density of a protoplanetary disk is  $n(\text{H}) = 10^{11} \text{ cm}^{-3}$  in the innermost region where the conditions are most favorable (Aikawa & Nomura 2006; Jonkheid et al. 2007). The carbon density including all atoms and molecules combined together is  $n(\text{C}) = 10^7 \text{ cm}^{-3}$  assuming nominal fractional abundance of carbon in the ISM. If we scale the growth rate of diamond in CVD formation on a warm substrate  $80 \mu\text{m hr}^{-1}$  (Angus & Hayman 1988) to the carbon abundance of a protoplanetary disk to a carbon star, a diamond particle in a protoplanetary disk could possibly grow to 200 nm in 1 Myr, which is about the size that we expect the diamond particles are in Elias 1. However, this is overly an optimistic estimate where no carbon atoms are locked in carbon monoxide, and all available for the diamond formation. In reality, the most abundant hydrocarbon  $\text{C}_2\text{H}$  in a protoplanetary disk is



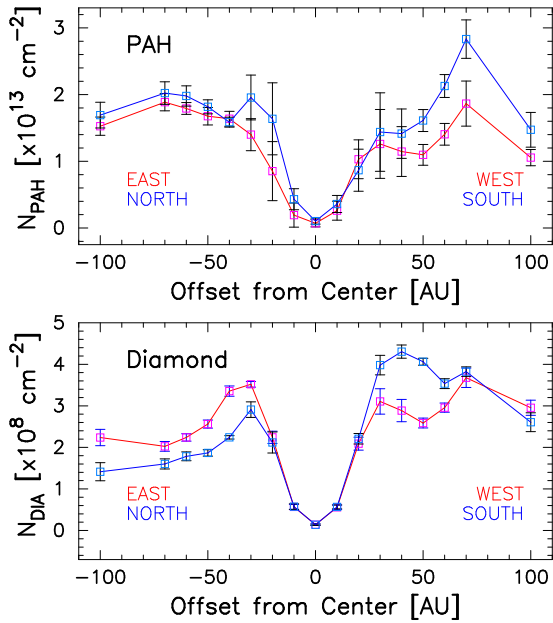


FIG. 4.— The radial profiles of the surface density of PAH and diamonds.

expected to be an order of 6–8 less than the total carbon abundance [ $n(\text{C}_2\text{H}) \approx 10^{-1} \text{ cm}^{-3}$ ]. Moreover, the growth rate implied by the homogeneous nucleation by Frenklach et al. (1989a) is  $10 \text{ nm hr}^{-1}$ , which is 3 orders of magnitude lower than we assumed above.

Nevertheless, in contrast to PAHs and silicates commonly observed both in disks and in the ISM, no diamonds emission or absorption has been ever detected in the diffuse ISM, which strongly implies that the diamonds in Elias 1 are formed *in situ*. Dai et al (2002) argued that the depletion of diamond particles in certain types of interplanetary dust is evidence that some diamonds are formed in the inner solar nebula. Even though the diamonds in the solar system is indeed presolar origin, that causes no contradiction with the diamond in Elias 1 being formed in the protoplanetary disk, as they may not have a common origin in the first place. The diamond particles extracted from meteorites are relatively small, between 1–10 nm in diameter (e.g., Bernatowicz et al. 1990), while the particle size of diamonds in Elias 1 and HD 97048 is at least one order of magnitude larger. Moreover, only 3 Herbig Ae/Be stars among more than 60 investigated show clear diamond emission features. There is no way to argue that diamond formation in the disks of Elias 1 and other Herbig Ae/Be stars is something other than an exception.

#### 4.2. Diamonds in the ISM and Protoplanetary Disks

##### 4.3. The Carbon Onion as a Pressure Cell

We propose here a diamond formation route in a protoplanetary disk using carbon onions as the high-pressure cell. The obvious problem in forming diamonds in a protoplanetary disk is how to maintain high pressures ( $>1 \text{ GPa}$ ; Bundy 1989), because graphite is otherwise energetically more favorable when the particles are macroscopic size. Banhart & Ajayan (1996) and Banhart (1997) produced carbon onions from nanometer-sized

graphite particles by the application of electron beams ( $1.25 \text{ MeV}$ ;  $200 \text{ A cm}^{-2}$ ). The carbon onions made in this way have concentric shells but with a spacing significantly smaller ( $0.31 \text{ nm}$ ) than in standard graphite material ( $0.34 \text{ nm}$ ). This is because the carbon atoms in the outer shells are knocked on during electron irradiation, and the outermost shells consequently shrink inward. The spacing of the shell becomes smaller in the inner part up to  $0.22 \text{ nm}$  at the center. The nucleus of the carbon onions therefore experiences enormous pressure estimated to be 50 to 100 GPa. The multiple onion-like shell therefore virtually provides a high-pressure cell required for diamond formation. Banhart & Ajayan (1996) further applied high-energy electron beams to the carbon onions and demonstrated that the cores of the carbon onions are indeed transformed into the lattice of the diamond within an hour or even faster.

It is not easy to show direct evidence of large carbon onions by astronomical observations because they should rather have a continuous absorption without bands or lines due to functional groups. There are no absorption measurements of such particles in laboratory because the perfect onions are only stable in the microscope under heating. Nevertheless, there are indications of carbon onions in the ISM from theory, laboratory experiments, and astronomical observations, though their sizes are not necessarily large. Tománek, Zhong, & Krastev (1993) has shown that when the size of the carbon cluster is more than 20 carbon atoms, a spherical multi-shell cluster is energetically most favorable among conic or cylindrical shells, or a single large shell. Laboratory experiments with resistively heated graphite rods by Schnaiter et al. (1998) and Jäger et al. (1999) have shown that the presence of hydrogen atoms like those in the ISM introduces curvature in the graphene planes, leading to the formation of an onion-like structure. The interstellar extinction curve shows a bump at  $217.5 \mu\text{m}$  with a remarkably stable central wavelength and narrow bump width. This might be also explained by carbon onions in the ISM according to the model calculation by Henrard, Lambin, & Lucas (1997) and Tomita, Fujii, & Hayashi (2004). Carbon onions have been found in meteorites (e.g. in Murchison by Amari et al. 1993). Although most of them are much smaller than  $100 \text{ nm}$ , the carbon onion particles found in Allende meteorite are as large as 10 to 50 nm (Smith & Buseck 1981).

Although we have only circumstantial evidence of large carbon onions in the ISM, they could also be formed in the same way as diamond under the electron or ion irradiation. Note that Banhart & Ajayan (1996) experiments do not start with carbon onions but are prepared beforehand from small graphite particles by electron irradiation. The transformation of carbon soot to multi-shell carbon particles (about  $50 \text{ nm}$  in diameter) under electron irradiation was also experimentally demonstrated by Ugarte (1992).

##### 4.4. Surfacing Diamond

The emission features at  $3.5 \mu\text{m}$  come from vibrational stretching of  $sp^3 \text{ C-H}$  bonds on the surface of diamond particles. Even if the diamond is formed in the core of the carbon onion pressure cell, the diamond emission features are not visible as long as it is shielded by the

onion shells. The diamond has to surface and be covered by ambient hydrogen atoms if the spectral features are to be observed.

The reversal of phase stability in diamond-graphite systems induced by irradiation offers a natural process for surfacing the diamonds. Zaiser & Banhart (1997) and Zaiser et al. (2000) have shown that once the diamond nucleates in the core of a carbon onion, the formation of diamond continues to the surface of the onion at the expense of the graphite shells until the entire carbon onion turns into a diamond particle. Graphite is more subject to displacement under the nonequilibrium state induced by constant particle irradiation, because of its lower threshold energy ( $\approx 10\text{--}20$  eV) than that of diamond ( $\approx 35$  eV; Zaiser & Banhart 1997). In an extreme circumstance where the carbon atoms are disturbed by uninterrupted particle impacts, the graphite shells are therefore gradually converted into diamond, which is the more stable form.

The most interesting aspect of the irradiation-induced phase transformation is that the displacement cross-section of graphite with respect to that of diamonds peaks at a temperature of  $\sim 600$  K (Zaiser et al. 2000). At that temperature the transition from graphite to diamonds does not require high pressure but proceeds as long as diamond nuclei exist (Lyutovich & Banhart 1999).

Low-mass stars during active accretion are hard X-ray sources, creating energetic particles required for diamond formation. However, diamond particles are only seen in warm disks around Herbig Ae/Be stars; none are found in T Tauri stars. This might be most simply understood in the same way as why fewer T Tauri stars show PAH emission than Herbig Ae/Be stars. Out of 54 pre-main sequence stars studied with *Spitzer*/IRS by Geers et al. (2006), 5 out of 9 Herbig Ae/Be stars show PAH emission, whereas only 3 out of 38 T Tauri stars do so. There might be plenty of diamonds in T Tauri disks, but we do not see them at all. This is because of insufficient radiation either to keep diamond particles in the warm disk atmosphere or to excite the C-H vibrational transition, as the effective temperatures of T Tauri stars ( $T_{\text{eff}} < 6000$  K) are lower than those of Herbig Ae/Be stars ( $T_{\text{eff}} \sim 10000$  K).

Another attractive explanation would be that the surfacing of diamond is hindered by the relatively cool disks of T Tauri stars where the stellar luminosity ( $L_* = 0.1\text{--}25 L_{\odot}$ ) is orders of magnitude less than that of Herbig Ae/Be stars. The surface area of the warm region in the disk ( $> 600$  K) where diamond formation proceeds without high pressure becomes smaller by a factor of 2–500 in T Tauri stars. The diamonds may exist in the grains in the disks of T Tauri stars, but they escape observation because they are covered under the mantles of carbon onions without C-H bonds on the surface to produce the diamond emission at  $3.53 \mu\text{m}$ . This might have consequence why the diamond particles sampled in the meteorites in the solar system are all small in the nanometer size (Lewis et al 1987).

#### 4.5. Origin of diamond

We present below a summary of diamond formation in the disk of Elias 1. The X-ray flares seen toward Elias 1 and MWC 297 originate from the magnetic activity of

low-mass companions. This is a signpost of the acceleration of high-energy particles. The presence of PAH emission, in contrast, suggests the presence of graphite, because the PAH molecules are physically and optically the low-mass end of the graphite particles (Draine & Li 2001). Although the exact route of the transformation is unclear, the anti-spatial correlation of PAH and diamond in Elias 1 implies the formation of diamonds from carbonaceous structures under the radiation of high-energy particles. van Kerckhoven, Tielens, & Waelkens (2002) analyzed the precise wavelength of the  $3.53 \mu\text{m}$  emission and concluded that the diamonds seen in HD 97048 are in a hot ambience around 1000 K (Lin et al. 1996). The temperature is somehow coincident with the ambient temperature of the experiment by Banhart & Ajayan (1996) (800 K) and the temperature required for surfacing diamond via irradiation-induced phase transformation ( $> 600$  K).

Elias 1 showed a large X-ray flare of  $L_X = 2.4 \times 10^{31} \text{ erg s}^{-1}$  with a duration of 10 ks during 120 ks observations by XMM *Newton* in 2001. A similar flare was also recorded by *Chandra* in 2002 (both reported in Giardino et al. 2004). The duration, duty cycle, peak energy flux, and the plasma temperature are statistically consistent with the flares seen in solar-type pre-main sequence stars (Feigelson et al. 2002; Wolk et al. 2005). A solar flare accelerates electrons above 20 keV that carry away a total of  $\sim 2 \times 10^{29}$  ergs in a single event while emitting a similar amount of energy in the soft X-ray regime ( $\sim 5 \times 10^{29}$  ergs; Lin 1974). About 0.1 % of the accelerated electrons reach the interplanetary space (Lin & Hudson 1971). If we scale the number of electrons produced in the solar flare to the flare in Elias 1 referring to  $L_X$ , and with the assumed differential spectral energy distribution with the power-law index  $\sim 3$  (Lin 1985; Krucker et al. 2007), the total electron emission more energetic than 1 MeV comes to  $4 \times 10^{24} \text{ erg s}^{-1}$ . The current influx ( $\sim 400 \text{ A cm}^{-2}$ ) that the carbon particles experience during a single event ( $\sim 3$  hr) are of the same order of magnitude as those of the experiment by Banhart & Ajayan (1996) ( $20\text{--}200 \text{ A cm}^{-2}$  for 1 hr) at the distance of 10 AU from Elias 1 where the temperature of disk atmosphere exceeds 1000 K (Aikawa & Nomura 2006; Jonkheid et al. 2007, warm enough to facilitate the irradiation-induced phase transformation). If we count in the protons and the heavy-ion nuclei, which are  $10^5$  to  $10^6$  times more efficient in transforming carbon onions to diamonds (Wesolowski et al. 1997), diamond nucleation and growth could take place even in the larger area of the protoplanetary disk.

We thank all the staff and crew of the Subaru Telescope for their valuable assistance in obtaining the data. We thank the anonymous referees for constructive criticism. Special thanks go to Manuel Güdel and Sigeo Yamachi for enlightening discussions on the X-ray nature of Herbig Ae/Be stars. We thank the anonymous referees for their constructive criticism. We appreciate the hospitality of the Hawaiian local community that made the research presented here possible. The Dark Cosmology Centre is funded by the Danish National Research Foundation. M.G. was supported by a fellowship from the Japan Society for the Promotion of Science.

## REFERENCES

- Acke, B., van den Ancker, M. E. 2006, *A&A*, 457, 171
- Aikawa, Y., & Nomura, H. 2006, *ApJ*, 642, 1152
- Allamandola, L. J., Sandford, S. A., Tielens, A. G. G. M., & Herbst, T. M. 1992, *A&A*, 399, 134
- Amari, A., Zimmer, E., & Leuws, R. S. 1993, *Meteoritics*, 28, 316
- Andersen, A. C., Jorgensen, U. G., Nicolaisen, F. M., Sorensen, P. G., & Glejbol, K. 1998, *A&A*, 330, 1080
- Angus, J. C., & Hayman, C. C. 1998, *Science*, 241, 913
- Asmann, M., Heberlein, J., & Pfender, E. *Diamond and Related Materials*, 1999, 8, 1
- Baidakova, M., & Vul'p, A. 2007, *J. Phys. D*, 40, 6300
- Banhart, F., & Ajayan, P. M. 1996, *Nature*, 382, 433
- Banhart, F. 1997, *J. Appl. Phys.* 81, 3440
- Berrilli, F., Corciulo, G., Ingrassio, G., Lorenzetti, D., Nisini, B., & Strafella, F. 1992, *ApJ*, 398, 254
- Bernatowicz, T. J., Gibbons, P. C., & Lewis, R. S. 1990, *ApJ*, 359, 246
- Bundy, F. P. 1989, *Physica A: Statistical and Theoretical Physics*, 158, 16
- Cheng, C.-L., Lin, J.-C., & Chang, H.-C. 1997, *J. Chem. Phys.*, 106, 7411
- Chiang, E. I., & Goldreich, P. 1997, *ApJ*, 490, 368
- Clayton, D. D., Meyer, B. S., Sanderson, C. I., Russell, S. S., & Pillinger, C. T. 1995, *ApJ*, 447, 894
- Cohen, M., & Kuhl, L. V. 1979, *ApJS*, 41, 743
- Dai, Z. R., Bradley, J. P., Joswiak, D. J., Brownlee, D. E., Hill, H. G. M., & Genge, M. J. 2002, *Nature*, 418, 157
- Daulton, T. L., Eisenhour, D. D., Bernatowicz, T. J., Lewis, R. S., & Buseck, P. R. 1996, *Geochim. Cosmochim. Acta.*, 60, 4853
- Damiani, F., Micela, G., & Sciortino, S. 2006, *A&A*, 447, 1041
- Draine, B. T. & Li, A. 2001, *ApJ*, 551, 807
- di Francesco, J., Evans, N. J., II, Harvey, P. M., Mundy, L. G., Guillobeau, S., Chandler, C. J. 1997, *ApJ*, 482, 433
- Dominik, C., Dullemond, C. P., Cami, J., & van Winckel, H. 2003, *A&A*, 397, 595
- Doucet, C., Habart, E., Pantin, E., Dullemond, C., Lagage, P. O., Pinte, C., Duchêne, G., & Ménard, F. 2007, *A&A*, 470, 625
- Dullemond, C. P., Henning, T., Visser, R., Geers, V. C., van Dishoeck, E. F., & Pontoppidan, K. M. 2007, *A&A*, 473, 457
- Dullemond, C. P., Dominik, C., & Natta, A. 2001, *ApJ*, 560, 957
- Elias, J. H. 1978, *ApJ*, 224, 857u
- Feigelson, E., Townsley, L., Güdel, M., & Stassun, K. 2007, *arXiv:astro-ph/0602603*
- Feigelson, E. D., Garmire, G. P., & Pravdo, S. H. 2002, *ApJ*, 572, 335
- Frenklach, M., Kematack, R., Huang, D., Howard, W., Spear, K. E., Phelps, A. W., & Koba, R. 1989a, *J. Appl. Phys.*, 66, 395
- Frenklach, M. 1989b, *J. Appl. Phys.*, 65, 5142
- Gaessler, W., et al. 2002, *Proc. SPIE*, 4494, 30
- Geballe, T. R., Noll, K. S., Whittet, D. C. B., & Waters, L. B. F. M. 1989, *ApJ*, 340, L29
- Geers, V. C., Augereau, J.-C., Pontoppidan, K. M., Dullemond, C. P., Visser, R., Kessler-Silacci, J. E., Evans, N. J., II, van Dishoeck, E. F., Blake, G. A., Boogert, A. C. A., Brown, J. M., Lahuis, F., & Mer, B. 2006, *A&A*, 459, 545
- Geers, V. C., van Dishoeck, E. F., Visser, R., Pontoppidan, K. M., Augereau, J.-C., Habart, E., & Lagrange, A. M.
- Ghez, A. M., McCarthy, D. W., Patience, J. L., & Beck, T. L. 1997, *ApJ*, 481, 378
- Giardino, G., Favata, F., Micela, G., & Reale, F. 2004, *A&A*, 413, 669
- Guillois, O., Ledoux, G., & Reynaud, C. 1999, *ApJ*, 521, L133
- Haas, M., Leinert, C., & Richichi, A. 1997, *A&A*, 326, 1076
- Habart, E., Testi, L., Natta, A., & Carillet, M. 2004a, *ApJ*, 614, L129
- Habart, E., Natta, A., & Krügel, E. 2004b, *A&A*, 427, 179
- Hamaguchi, K., Terada, H., Bamba, A. & Koyama, K. 2000, *ApJ*, 532, 1111
- Henning, T., Burkert, A., Launhardt, R., Leinert, C., & Stecklum, B. 1998, *A&A*, 336, 565
- Henrad, L., Lambin, P., & Lucas, A. A. 1997, *ApJ*, 487, 719
- Jäger, C., Henning, T., Schlögl, R., & Spillecke, O., *Non-Crystalline Solids*, 258, 161
- Jones, A. P., d'Hendecourt, L. B., Sheu, S.-Y., Chang, H.-C., Cheng, C.-L., & Hill, H. G. M. 2004, *A&A*, 416, 235
- Jonkheid, B., Dullemond, C. P., Hogerheijde, M. R., & van Dishoeck, E. F. 2007, *A&A*, 453, 203
- Jørgensen, R. 1998, *Nature*, 332, 702
- Kataza, H., & Maihara, T. 1991, *A&A*, 248, L1
- Kobayashi, N., Tokunaga, A. T., Terada, H., Goto, M., Weber, M., Potter, R., Onaka, P. M., Ching, G. K., Young, T. T., Fletcher, K., Neil, D., Robertson, L., Cook, D., Imanishi, M., & Warren, D. W. 2000, *Proc. SPIE*, 4008, 1056
- Kouchi, A., Nakano, H., Kimura, Y. & Kaito, C. 2005, *ApJ*, 626, L129
- Krucker, S., Kontar, E. P., Christe, S., & Lin, R. P., *ApJ*, 663, 109
- Kurucz, R. L. 1979, *ApJS*, 40, 1
- Lewis, R. S., Ming, T., Wacker, J. F., Anders, E. & Steel, E. 1987, *Nature*, 326, 160
- Li, A., & Draine, B. T. 2001, *ApJ*, 554, 778
- Lin, R. P., & Hudson, H. S., 1971, *Sol. Phys.*, 17, 412
- Lin, R. P. 1974, *Space Sci. Rev.*, 16, 189
- Lin, R. P. 1985, *Sol. Phys.*, 100, 537
- Lin, J. C., Chen, K. H., Chang, H. C., Tsai, C. S., Lin, C. E., & Wang, J. K. 1996, *J. Chem. Phys.* 105, 3975 Sue
- Liu, W. M., Hinz, P. M., Meyer, M. R., Mamajek, E. E., Hoffmann, W. F., Brusa, G., Miller, D. & Kenworthy, M. A. 2007, *ApJ*, 658, 1164
- Lord, S. D. 1992, *A New Software Tool for Computing Earth's Atmosphere Transmissions of Near- and Far-Infrared Radiation*, NASA Technical Memoir 103957 (Moffett Field, CA: NASA Ames Research Center)
- Lugaro, M., Pols, O., Karakas, A. I. & Tout, C. A. 2005, *Nucl. Phys. A*, 758, 725
- Lytovich, Y., & Banhart, F. 1999, *Appl. Phys. Lett.* 74, 659
- Malfait, K., Waelkens, C., Waters, L. B. F. M., Vandenbussche, B., Huygen, E., & de Graauw, M. S. 1998, *A&A*, 332, L25
- Meeus, G., Waters, L. B. F. M., Bouwman, J., van den Ancker, M. E., Waelkens, C., & Malfait, K. 2001, *A&A*, 365, 476
- Men'shchikov, A. B., Henning, T. 1997, *A&A*, 318, 879
- Mutschke, H., Andersen, A. C., Jäger, C., Henning, T., & Braatz, A. 2004, *A&A*, 423, 983
- Nuth, J. A. III, & Allen, J. E. Jr. 1992, *Ap&SS*, 196, 117
- Schnaiter, M., Mutschke, H., Dorschner, J., Henning, T., & Salama, F. 1998, *ApJ*, 498, 486
- Schutte, W. A., Tielens, A. G. G. M., Allamandola, L. J., Wooden, D. H., & Cohen, M. 1990, *ApJ*, 360, 577
- Sheu, S.-Y., Lee, I.-P., Lee, Y. T., & Chang, H.-C. 2002, *ApJ*, 581, L55
- Smith, P. P. K., & Buseck, P. 1981, *Science*, 212, 322
- Smith, K. W., Balega, Y. Y., Duschl, W. J., Hofmann, K.-H., Lachaume, R., Preibisch, T., Schertl, D., & Weigelt, G. 2005, *A&A*, 431, 307
- Stelzer, B., Micela, G., & Neuhäuser, R. 2004, *A&A*, 423, 1029
- Stelzer, B., Micela, G., Hamaguchi, K., & Schmitt, J. H. M. M. 2006, *A&A*, 457, 223
- Strom, K. M., & Strom, S. E. 1994, *ApJ*, 424, 237
- Takami, H., et al. 2004, *PASJ*, 56, 225
- Terada, H., Imanishi, M., Goto, M. & Maihara, T. 2001, *A&A*, 377, 994
- Thé, P. S., de Winter, D., & Pérez, M. R. 1998, *A&AS*, 104, 315
- Tielens, A. G. G. M., Seab, C. G., Hollenbach, D. J., & McKee, C. F. 1987, *ApJ*, 319, L109
- Tokunaga, A. T., Kobayashi, N., Bell, J., Ching, G. K., Hodapp, K.-W., Hora, J. L., Neill, D., Onaka, P. M., Rayner, J. T., Robertson, L., Warren, D. W., Weber, M., & Young, T. T. 1998, *Proc. SPIE*, 3354, 512
- Tománek, D., Zhong, W., & Krastev, E. 1993, *Phys. Rev. B*, 48, 15461
- Tomita, S., Fujii, K. M., & Hayashi, S. 2004, *ApJ*, 509, 220
- Topalovic, R., Russell, J., McCombie, J., Kerr, T. H., & Sarre, P. J. 2006, *MNRAS*, 372, 1299
- Ugarte, D. 1992, *Nature*, 359, 707
- van Boekel, R., Waters, L. B. F. M., Dominik, C., Dullemond, C. P., Tielens, A. G. G. M., & de Koter, A. 2004, *A&A*, 418, 177
- van Kerckhoven, C., Tielens, A. G. G. M., & Waelkens, C. 2002, *A&A*, 384, 568
- Visser, R., Geers, V. C., Dullemond, C. P., Augereau, J.-C., Pontoppidan, K. M., & van Dishoeck, E. 2007, *A&A*, 466, 229
- Vink, J. S., O'Neill, P. M., Els, S., & Drew, J. E. 2005, *A&A*, 438, 21
- Waelkens, C., Waters, L. B. F. M., de Graauw, M. S., Huygen, E., Malfait, K., Plets, H., Vandenbussche, B., Beintema, D. A., Boxhoorn, D. R., Habing, H. J., Heras, A. M., Kester, D. J. M., Lahuis, F., Morris, P. W., Roelfsema, P. R., Salama, A., Siebenmorgen, R., Trams, N. R., van der Blik, N. R., Valentijn, E. A., & Wesselius, P. R. 1996, *A&A*, 315, L245
- Whittet, D. C. B., Williams, P. M., Zealey, W. J., Bode, M. F., & Davies, J. K. 1983, *A&A*, 121, 301
- Whittet, D. C. B., McFadzean, A. D., & Geballe, T. R. 1984, *MNRAS*, 211, 29
- Wesolowski, P., Lyutovich, Y., Banhart, F., Carstensen, H. D., & Kronmüller, H. 1997, *Appl. Phys. Lett.* 71, 3439
- Wdowiak, T. J. 1987, *Nature*, 328, 385
- Wolk, S. J., Harnden, F. R., Jr., Flaccomio, E., Micela, G., Favata, F., Shang, H., & Feigelson, E. D. 2005, *ApJS*, 160, 423
- Zaiser, M., & Banhart, F. 1997, *Phys. Rev. Lett.* 79, 3680
- Zaiser, M., Lyutovich, Y. & Banhart, F. 2000, *Phys. Rev. B*, 62, 3058
- Zinnecker, H., & Preibisch, T. 1994, *A&A*, 292, 152